Yehua TANG[1,2], Chunlana ZHOU[1*], Wenjing WANG[1], Su ZHOU[1,2], Yan ZHAO[1,2], Xiangxin LIU[1], Lei ZHAO[1], Hailing LI[1], Jingwei CHEN[1,2], Baojun YAN[1,2], Jianming FEI[3], Hongbin CAO[3], Xin WU[4]

1 Institute of Electrical Engineering, Key Laboratory of Solar Thermal Energy and Photovoltaic Systems, Chinese Academy of Sciences, Beijing 100190, P. R. China
2 Graduate University of the Chinese Academy of Sciences, Beijing 100049, P. R. China
3 Eoplly New Energy Technology Co., Ltd. Nantong, Jiangsu 226602, P. R. China, 4 Beijing NMC Co., Ltd., Beijing 100015, P. R. China

EL and ITG Characterization of Large Areas Black Silicon Solar Cells VIA Screen Printing

Abstract*. A simple process of texturing silicon (Si) surfaces using gold (Au)-catalyzed wet chemical etching was used to form black Si (BS) on a (100) p-type substrate. The surface became uniformly black after 6 min, with a resulting reflectivity of < 2% over the 400 nm to 1100 nm wavelength range. Large areas (153.18 cm2) of black Si solar cells (BSSCs) with an n+-p-p+ structure were also fabricated using conventional processes, including POCl3 diffusion, screen printing, and co-firing. The resulting cells were divided into two groups according to the emitter (46 and 37 Ω/□), and their output parameters were studied. The best convention efficiency (Eff) was < 10%. The open-circuit voltage (Voc) was particularly low because of poor surface passivation, and the shunt resistance (Rsh) linearly decreased with the series resistance (Rs). Electroluminescence (EL) and infrared thermography (ITG) measurements were conducted to characterize the BSSCs. Both the emissivity and temperature were low and non-uniform. Optimizing the fabrication process by reducing the etching depth and lowering the dopant sheet resistance led to significant improvement in Voc (~48 mV) and Eff (~3.8% absolute). EL and ITG measurements indicate that Rs is another important factor that accounts for the poor properties of the BSSCs.*

Streszczenie: *Do wytworzenia czarnego krzemu (BS) na podłożu typu p-Si(100) zastosowano prosty sposób teksturowania powierzchni krzemowej metodą chemicznej akwaforty na mokro z zastosowaniem, jako katalizatora, nanocząstek złota (Au). Podłoże staje się jednolicie czarne po 6 min, osiągając współczynnik odbicia < 2% w zakresie długości fali od 400 nm do 1100 nm. Wykonano również dużą powierzchnię czarnych krzemowych ogniw słonecznych (BSSC), ze strukturą n^+ - p -n^+, konwencjonalnymi metodami obejmującymi dyfuzję POC13,drukowanie maski i wyżarzanie. Otrzymane ogniwa dzielą się na dwie grupy w zależności od emitera (46 i 37Ω/□): zbadano ich wyjściowe parametry. Najlepsza uzyskana wydajność wynosi < 10%. Napięcie obwodu otwartego (Voc) jest szczególnie niskie z powodu słabej pasywacji powierzchni, a rezystancja równoległa (Rsh) liniowo maleje z rezystancją szeregową (Rs). Charakterystykę BSSC określają pomiary elektroluminescencji (EL) i tomografii w podczerwieni (ITG).Zarówno emisyjność jak i temperatura są niskie i niejednorodne. Optymalizacja procesu wykonana przez zmniejszenie głębokości akwaforty i obniżenie rezystancji warstwy domieszkowania prowadzi do znaczącej poprawy Voc (ok. 48mV) i Eff (ok. 3,8%).****Ocena EL i ITG czarnych krzemowych ogniw słonecznych o dużej powierzchni wykonanych przez drukowanie maski***

Keywords: Black Si solar cells, Au catalysis, EL measurement, ITG test.
Słowa kluczowe: Czarne krzemowe ogniwa słoneczne**,** Kataliza Au, pomiary elektroluminescencji (EL), Test tomografii w podczerwieni

1. Introduction

Pyramid-shaped structures can be formed on silicon (Si) surfaces using a potassium hydroxide (KOH) solution. KOH is widely used in the Si solar cell manufacturing process to achieve a weighted reflectivity of approximately 13%. Reducing the surface reflectance is an effective method of obtaining high-efficiency cells. Hence, a simple process of preparing antireflective surfaces and integrating such surfaces into Si solar cells must be developed. Simulation results reported by Sai et al.1 showed that the subwave structure (SWS), known as black silicon (BS), has a low mean reflectivity (below 3%) improvement (25% to 42%) in the short-circuit current silicon solar cells (BSSCs) were fabricated, a significant (Isc) 7,8 was achieved with the antireflective BS structure. Other performance parameters, such as the open-circuit voltage (Voc) and fill factor (FF), were not affected. In 2009, Yuan et al. 9 fabricated BSSCs on a 1 cm2 floating zone (FZ) p-Si (100) substrate. The surface passivation layer was thermally deposited SiO2, and the front electrode was prepared via photolithography and evaporation of Ti/Pd/Ag. A maximum efficiency (Eff) of 16.8% was achieved without any antireflective coating. Photolithography, thermal oxidation, and evaporation are widely used at the laboratory scale to prepare high Eff Si solar cells, but they are not suitable for industrial application because of their high cost and complexity. A fast and simple process of preparing large-area (153.18 cm2) BS surfaces was developed using Au nanoparticle-catalyzed wet chemical etching in aqueous hydrogen fluoride (HF) and hydrogen peroxide (H2O2) at room temperature. The reflectivity over the 400 nm to 1100 nm wavelength range was < 2%. BSSCs with different dopant profiles were also fabricated via conventional processes, such as phosphoryl chloride (POCl3) diffusion, commercial paste screen-printing, and co-firing. Electroluminescence (EL) and infrared thermography (ITG) measurements10–14 showed that a lower sheet resistance is beneficial for cells. The Voc and FF of these cells were particularly low, and the best Eff was < 10%. Optimizing the fabrication process by reducing the etching depth and changing the dopant profile led to an Eff enhancement of ~3.8% (abs.) and a Voc enhancement of ~48 mV.

2. Materials and Methods

Samples were prepared from 180 μm thick, commercially available (100) p-type Czochralski (CZ) silicon wafers (~1.5 □cm, boron-doped). The samples were initially polished using HF and nitric acid (HNO3) to remove the layer damaged by the saw wires. The samples were then thoroughly rinsed with deionized (DI) water. The samples were dipped into 0.4 mmol/L chloroauric acid (HAuCl3) mixed with polyethyleneimine (PEI)15, 16 for 2 min at room temperature to allow the deposition of the Au nanoparticle layer on the Si substrate. The initial PEI:HAuCl3 molar ratio was 4:1. The samples were subsequently immersed in an etching solution of HF, hydrogen peroxide (H2O2), and DI water (HF:H2O2:H2O = 1:5:10) at room temperature for 6 min. The etching mechanism was as follows: $Si + H_2O_2 + 6HF \rightarrow 2H_2O + H_2SiF_6 + H_2\uparrow$. The samples were then rinsed with DI water, and the residual Au nanoparticles were removed from the reaction mixture2 by adding I2:NH4I:H2O = 1:4:40 at 80 ° C for 5 min. Finally, the samples were rinsed with DI water, blown dry with nitrogen, and subjected to further investigation. Reflectivity measurements were performed using a “Solar Cell Spectral Responser/QE/IPCE Measuement System” (Model: QEX 7) over the 300 nm to 1200 nm wavelength range.

BSSCs were fabricated in the production line. BS samples were initially immersed in chloroazotic acid at 80 °C for ~20 min to remove any Au residue prior to BSSC fabrication. After a standard RCA cleaning, the emitter diffusion was prepared in POCl3 in a tube furnace. Two different emitters were used, namely, a high-ohmic emitter with a mean sheet resistance (R) of 46 /□and a low-ohmic emitter with R= 37/□. The latter was diffused through a reference cell, which was etched with aqueous KOH along the line (pyramid-structure surface). The R□ value was 46 /□. After edge isolation and phosphosilicate glass removal, a SiNx layer (n=2.05, 80 nm), acting as an antireflection coating and passivation layer, was deposited via plasma-enhanced chemical vapor deposition. Both the rear and front metal contacts were fabricated using screen-printing commercial paste and through a co-firing process in an infrared conveyor belt furnace.

The electrical characterization of BSSC and the reference cells were performed using an I-V and spectral response system (Model: XJCM-9) under an AM 1.5 G spectral irradiance (100 mW/cm2 at 25 °C). EL and ITG mapping of the solar cells were conducted using a commercial mapping system. Optimized BSSCs were fabricated by reducing the etching time to 4 min, which in turn reduced the etching depth. Two different emitters, 46 and 31/were used.

3. Results and Discussion

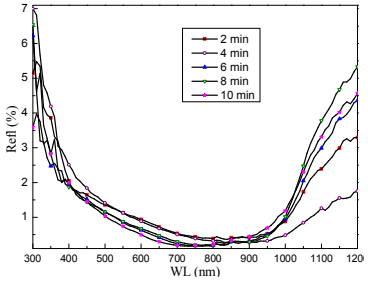

Fig. 1. Reflectivity versus wavelength curve of etched black silicon (BS) surfaces at the different Au nanoparticle deposition times (ADT)

Table 1. Weighted reflectivity (R) of BS in random cones and pyramid samples at different ADTs.

Surface structure	ADT (min)	T (min)	Solution	R (%)
pyramid	-	28	KOH	13.60
random cones	2	6	HF, H2O2, H2O	1.56
random cones	4	6	HF, H2O2, H2O	1.45
random cones	6	6	HF, H2O2, H2O	1.24
random cones	8	6	HF, H2O2, H2O	1.26
random cones	10	6	HF, H2O2, H2O	1.23

The reflectivity of the BS structures versus the wavelength at different Au deposition times (ADT) was investigated. Fig. 1 shows the reflectivity versus wavelength curves of all samples at different ADTs and at 6 min etching time. The weighted reflectivities (R) are summarized in Table 1, including that of a reference sample etched in a KOH solution at 80 °C for ~25 min. The reflection spectrum of the BS surface exhibited a typically low reflectivity (< 2%), particularly in the 400 nm to 1100 nm wavelength range. The morphology of the etched BS surface resembled random cones (data to be published elsewhere), and the width and depth were approximately 10 and 250 nm, respectively. Fig. 1 shows that the reflectivity varied with ADT, which may be due to the Au nanoparticle coverage rate. A longer deposition time allows a higher coverage rate and decreased surface reflectivity with increasing ADT.

In summary, a fast and simple process of preparing nanoporous Si-structured BS surfaces using Au-catalyzed wet chemical etching (in aqueous HF and H2O2) was demonstrated, and a low-weighted reflectivity (~1.5%) surface was achieved.

The minority carrier lifetime (τ) was measured using Semilab-2000 to evaluate the effect of Au. τ was ~15 μs for BS and ~13 μs for the reference cell, indicating the absence of Au contamination in the BS emitter layer.

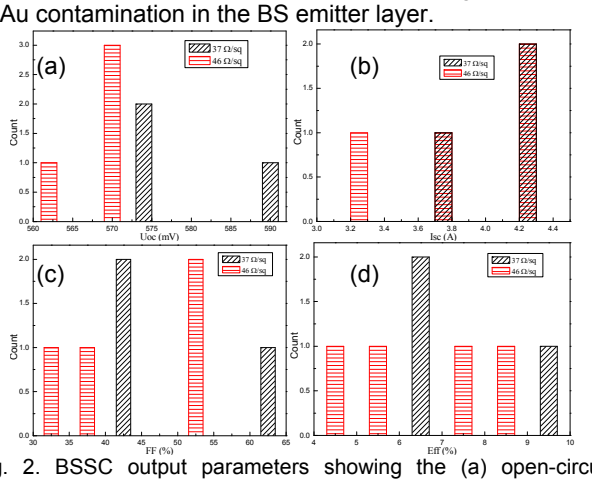

Fig. 2. BSSC output parameters showing the (a) open-circuit voltage, Voc; (b) short-circuit current, Isc; (c) fill factor, FF; and (d) efficiency, Eff distributions

Fig. 2 shows the illuminated output parameter (Voc, Isc, FF, and Eff) distributions of the cells prepared on BS substrates with different dopant profiles. All parameters of the heavier dopant samples increased, especially Voc. The best Eff for the 46 / samples was 8.39%, whereas that of the 37 /□samples was 9.43%. The average Eff value of 50 reference cells was 17.2%. Detailed comparisons of the other electrical properties (including dark I-V and QE) of the BSSCs and the reference samples were also performed, and the results will be published elsewhere. The BSSC properties were inferior to those of the reference cells, especially Voc and FF, possibly because the BS layer acted as a recombination layer9 to reduce Voc. Thus, the BS layer cannot be efficiently passivated by a SiNx film. The series resistance (Rs) and shunt resistance (Rsh) were the primary reasons for the poor FF. The Rsh versus Rs curves of all BSSCs (Fig. 3) clearly shows that Rsh linearly decreased with Rs. This decrease may have been due to the high peak temperature during the firing process, or the BS structure itself. The BS layer is a nanoporous structure with a significantly increased superficial area, which allowed the easy etching of the Ag paste.

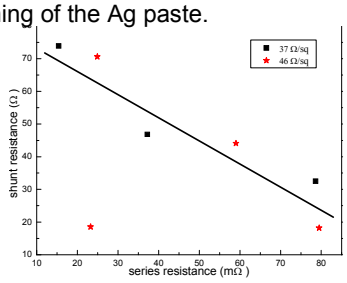

Fig. 3. Rsh versus Rs curve for the BSSCs

EL and ITG measurements were conducted to further investigate the characteristics of the BSSCs. The spatial variations in the emissivity of the different dopant BSSCs and reference cells under a 5 A forward current in the dark are shown in Fig. 4 The corresponding temperature distributions are shown in Fig. 5.

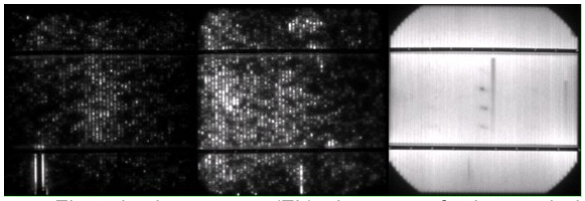

Fig. 4. Electroluminescence (EL) images of the emissivity distribution measured at a 5 A forward current: (a) 46, (b) 37, and (c) 46 Ω/□ reference cell

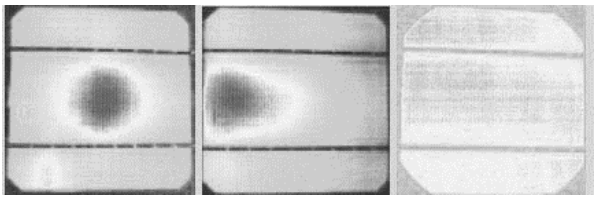

Fig. 5. Temperature distribution of the ITG images measured at a 5 A forward current: (a) 46 Ω/□ BSSC, (b) 37 Ω/□ BSSC, and (c) 46 Ω/□ reference cell

The reference cell exhibited a homogeneous emissivity (Fig. 4c), except for a few disconnected fingers and conveyors and a uniform temperature (Fig. 5c). The EL of the BSSCs was largely dark (Figs. 4a and 4b) and the temperature distribution was non-uniform compared with those of the reference. A careful comparison between Figs. 4a and 4b reveals an emissivity enhancement in the 37 Ω/□ cell. A heavier dopant (lower emitter sheet) enhances BSSC performance. In addition, a comparison between Figs. 4 and 5 shows that the temperature was higher for the brighter areas in the EL image of the BSSCs. Hence, Rs was the dominant factor that caused the lower emission intensity of the BSSCs17, indicating that the BSSCs benefited from the heavier dopant. The EL measurements for the BSSCs under a 12 V reverse bias in the dark were also performed, and the resulting images are all dark (data not shown).

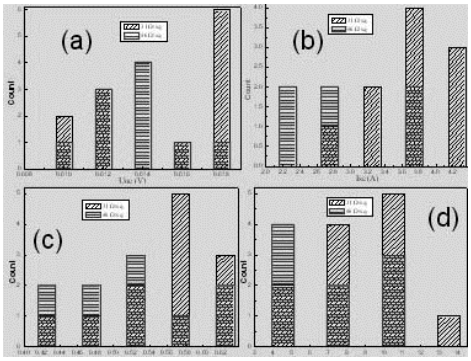

Fig. 6. Optimized BSSC output parameters showing the (a) Voc, (b) Isc, (c) FF, and (d) Eff distributions

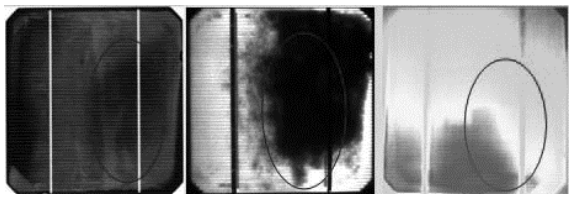

Fig. 7. Images of the 46 Ω/□ BSSC after 4 min etching : (a) front side, (b) emissivity distribution of the EL image measured at a 5 A forward current, and (c) ITG temperature distribution measured at a 5 A forward current

In summary, low-weighted reflectivity BS structure surfaces were obtained via catalysis with Au nanoparticles. Au is well known for shortening the minority carrier lifetime; thus, its presence must be prevented via careful cleaning. The performance of the BSSC cells was poor compared with that of the reference cells etched by KOH, and a heavier emitter dopant improved the performance of the BSSCs. The present section focuses on BSSC fabrication optimization to improve the BSSC properties. As previously noted, (i) the BS layer acted as a dead layer, whereas the thicker layer exhibits a greater effect; thus, the Voc of the BSSCs was lower than that of the reference cells; and (ii) a heavier emitter dopant is beneficial to BSSCs. The etching depth was reduced by shortening the etching time to 4 min to reduce the surface recombination velocity. The BSSCs were then fabricated, and two different dopant profiles (46 and 31 Ω/□) were obtained.The BSSC output parameters are shown in Fig. 6. In general, the BSSC properties were significantly improved, especially Voc. The 46 Ω/□ based cell samples etched for 4 min showed improved properties. The best Eff for the samples etched for 4 min was 11.33%, and the Voc was 610 mV, compared with the 8.39% and 570 mV of the samples etched for 6 min, respectively.

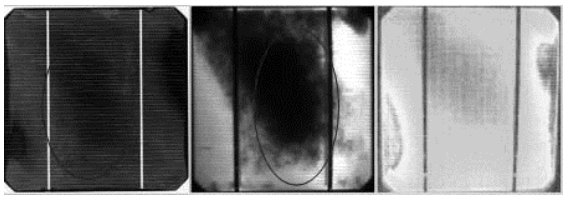

Fig. 8. Images of the 31 Ω/□ BSSC after 4 min etching: (a) front side, (b) emissivity distribution of the EL image measured at a 5 A forward current, and (c) ITG temperature distribution measured at a 5 A forward current

In the samples etched for 4 min, the 31 Ω/□ solar cells exhibited the best performance, with a maximum Eff of 12.17% and a Voc of 618 mV, indicating improved Eff (~3.8% abs.) and Voc (~47.9 mV). On the other hand, the Isc and FF of the 31 Ω/□ 4 min etched sample was 4.73 A and 64.5%, respectively, compared with the 4.37 A and 52.2% of the 6 min etched 46 Ω/□ samples. BS has a nanoporous structure that increases the superficial area and acts as a dead layer. The shortened etching time reduced the etching depth and surface recombination; hence, Voc was significantly improved. Voc remained lower than that of the reference cell (~620 mV) because of the poor surface passivation. Although Isc and FF were also affected by surface recombination, they slightly improved with the reduction in etching time, mainly because of Rs and Rsh. EL and ITG measurements were performed to verify the results of the BSSCs fabricated at different etching times and using different dopant emitters. In particular, the reason for the lower Isc and FF values was sought.

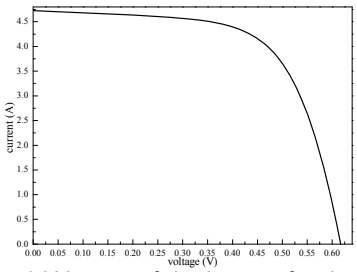

Fig. 9. Illuminated I-V curve of the best performing optimized BS cell

Fig. 7 shows the front side of the EL and ITG images of the 4 min etched 46 Ω/□ sample, whereas those of the 4 min etched 31 Ω/□ sample are shown in Fig. 8. Reducing the etching time led to higher EL emissivities. However, a uniform black surface was difficult to obtain because of the

large area (Figs. 7 and 8). The emission intensity and temperature of the black region at the front side (marked by red circles) were lower. The Rs in the black region was particularly high17, as verified by the illuminated I-V curve (Fig. 9), possibly due to the firing process.

Gaps in the processing, which include the modification of the etching solution, the firing process, and related aspects, will form the bases of future studies.

2. Conclusions

Nanoporous subwave BS structures in random cones were formed via a wet chemical etching method catalyzed by Au nanoparticles. The reflectivity in the 400 nm to 1100 nm wavelength range was < 2%, and the BS exhibited favorable light-trapping properties. After etching the BSSC for 6 min, the resulting properties were much lower than those of the reference cell. EL and ITG measurements indicate that Rs was the main reason for this observation. Rsh linearly decreased with Rs. However, BSSCs can benefit from heavier doping emitters. Reducing the etching time to 4 min significantly improved the output properties. An improvement in Voc (~48 mV) and Eff (~3.8% abs.) was observed for the 31/ solar cells compared to their 46/□ analogue. Other parameters also improved with shallower etching depths and lower dopant emitter contents. The output parameters and the EL and ITG measurements indicate that the properties of the optimized BSSCx were significantly improved.

Acknowledgments

Supported by the Knowledge Innovation Program of the Chinese Academy of Sciences (Grant No. KGCX2-YW-382) and the National Program for Key Basic Research Project (Grant No. 2010CB933804).

REFERENCES

1. H. Sai, H. Fujii, et al., Numerical analysis and demonstration of submicron antireflective textures for crystalline silicon solar cells, Photovoltaic Energy Conversion, Conference Record of the 2006 IEEE 4th World Conference on (2006), pp. 1191–1194.
2. K. Nishioka, S. Horita, et al., Antireflection subwavelength structure of silicon surface formed by wet process using catalysis of single nano-sized gold particle, Solar Energy Materials and Solar Cells, vol. 92, (2008), pp. 919–922.
3. S. Koynov, M. S. Brandt, et al., Metal-induced seeding of macropore arrays in silicon, Advanced Materials, vol. 18, (2006), pp. 633–+.
4. T. K. Sarma, D. Chowdhury, et al., Synthesis of Au nanoparticle-conductive polyaniline composite using H2O2 as oxidising as well as reducing agent, Chemical Communications, (2002), pp. 1048–1049.
5. K. Tsujino, M. Matsumura, et al., Texturization of multicrystalline silicon wafers by chemical treatment using metallic catalyst, 2003.
6. K. Tsujino, M. Matsumura, et al., Texturization of multicrystalline silicon wafers for solar cells by chemical treatment using metallic catalyst, Solar Energy Materials and Solar Cells, vol. 90, (2006), pp. 100–110.
7. S. Koynov, M. S.Btandt, et al., Black multi-crystalline silicon solar cells, PHYSICA STATUS SOLIDI-RAPID RESEARCH LETTERS, vol. 1, (2007), pp. R53–R55.
8. K. Nishioka, T. Sueto, et al., Antireflection structure of silicon solar cells formed by wet process using catalysis of single nano-sized gold or silver particle, Photovoltaic Specialists Conference (PVSC), 2009 34th IEEE (2009), pp. 169–171.
9. H.-C. Yuan, V. E.Yost, et al., Efficient black silicon solar cell with a density-graded nanoporous surface: Optical properties, performance limitations, and design rules, Applied Physics Letters, vol. 95, (2009), pp. 123501–123503.
10. 1K. Bothe, K. Ramspeck, et al., Luminescence emission from forward- and reverse-biased multicrystalline silicon solar cells, Journal of Applied Physics, vol. 106, (2009), pp. 104510-1-104510-8.
11. O. Breitenstein, J. Bauer, et al., On the detection of shunts in silicon solar cells by photo- and electroluminescence imaging, Progress in Photovoltaics, vol. 16, (2008), pp. 325–330.
12. T. Fuyuki, H. Kondo, et al., "One shot mapping of minority carrier diffusion length in polycrystalline silicon solar cells using electroluminescence," in Conference Record of the Thirty-First IEEE Photovoltaic Specialists Conference - 2005, ed, 2005, pp. 1343–1345.
13. M. Glatthaar, J. Giesecke, et al., Spatially resolved determination of the dark saturation current of silicon solar cells from electroluminescence images, Journal of Applied Physics, vol. 105, (2009), pp. 113110-1-113110-5.
14. D. Hinken, K. Ramspeck, et al., Series resistance imaging of solar cells by voltage dependent electroluminescence, Applied Physics Letters, vol. 91, (2007), pp. 182104-1-182104-3.
15. 1X. Sun, S. Dong, et al., One-step polyelectrolyte-based route to well-dispersed gold nanoparticles: Synthesis and insight, Materials Chemistry and Physics, vol. 96, (2006), pp. 29–33.
16. C. Chen and P. Kuo, Gold nanoparticles prepared using polyethylenimine adsorbed onto montmorillonite, Journal of Colloid and Interface Science, vol. 293, (2006), pp. 101–107.

Authors*: dr inż. Yehua Tang, Institute of Electrical Engineering, Key Laboratory of Solar Thermal Energy and Photovoltaic Systems, Chinese Academy of Sciences, Beijing 100190, P. R. China, E-mail: asiantangyehua@163.com; dr inż, Chunlana Zhou, Institute of Electrical Engineering, Key Laboratory of Solar Thermal Energy and Photovoltaic Systems, Chinese Academy of Sciences, Beijing 100190, P. R. China, email: chunlzhou@gmail.com*.